Journal of
Electronic Imaging

SPIEDigitalLibrary.org/jei

Uneven illumination removal and image enhancement using empirical mode decomposition

Soo-Chang Pei
Yu-Zhe Hsiao
Mary Tzeng
Feng Ju Chang

SPIE

IS&T
imaging.org

Journal of Electronic Imaging 22(4), 043037 (October 2013)

Uneven illumination removal and image enhancement using empirical mode decomposition

Soo-Chang Pei, Yu-Zhe Hsiao,* Mary Tzeng, and Feng Ju Chang
National Taiwan University, Graduate Institute of Communication Engineering, No. 1, Section 4, Roosevelt Road, Taipei 10617, Taiwan

Abstract. Uneven light distribution problems often arise in poorly scanned text or text-photo images and natural images taken by digital camera. An innovative image-processing technique for uneven illumination removal using empirical mode decomposition (EMD) is proposed. The EMD is local, adaptive, and useful for analyzing nonlinear and nonstationary signals. In this method, we decompose images by EMD and get the background level locally and adaptively. This algorithm can enhance the local reflectance in the image while removing uneven illumination for black/white text images, text-photo images, and natural color/gray-level images. The proposed technique can be very helpful for image and text recognition. The EMD can also be applied to the three color channels (RGB) of color images separately to estimate the reflectances of the three color channels. After we relight these channels using white light and the estimated reflectances, a simple color constancy task can be performed to correct certain poorly lighted color images. Our technique is compared with recently proposed methods for correcting images with uneven illumination and the experimental results demonstrated that the proposed approach can effectively enhance natural color/gray-level images and make text and text-photo images more readable under uneven illumination. [DOI: 10.1117/1.JEI.22.4.043037]

Keywords: image enhancement; image processing; imaging; uneven illumination removal.

Paper 13002 received Jan. 2, 2013; revised manuscript received Oct. 11, 2013; accepted for publication Nov. 21, 2013; published online Dec. 20, 2013.

1 Introduction

With the digitization of scientific and technological products in recent years, more and more devices need image processing skill, including digital still cameras (DSC), cell-phones, projectors, printers, liquid crystal TVs, LCDs, video presentation systems (VPS), etc. All of these devices need to show good-looking images. The DSCs are used to take pictures just like conventional film cameras. People prefer digital cameras over traditional cameras for their convenience. However, in many situations, the cameras are unable to work well in darker environments or with uneven light sources. Figure 1(a) shows an example of color image with a shadow on its right side and the source luminance on the left side. We would like to make this image more pleasing by applying image processing techniques. With the development of computer technology and the internet, we often want to digitize our documents to facilitate their storage and distribution by using a scanner. However, poorly scanned text and text-photo images like those demonstrated in Figs. 1(b) and 1(c) are often encountered. Due to the uneven light distributions (LDs) shown in Figs. 1(b) and 1(c), we cannot see the details clearly, and it is difficult to read the text in the shadow of the images.

Many algorithms have been proposed to solve the uneven illumination removal problem of images in the literature. In what follows, we briefly review those methods proposed in recent years. The well-known histogram equalization algorithm may be the simplest and most straightforward way to correct images with uneven LD. On the other hand, the enhanced results depend strongly on LD in original images. It works well for images with global low contrast, but it is not suitable for images with local low contrast. Therefore, we seldom can obtain satisfactory results and uneven LD still exists in most of the enhanced results. In 2005, Hsia and Tsai[1] came up with a method called "efficient light balancing techniques (ELBT)" to correct the uneven illuminated images for VPS application. However, the ELBT is only suitable for processing black/white text images and its range of applications is limited. Consequently, in 2006, Hsia and Tsai[2] again proposed the "line-based light-balancing algorithm (LLBT)" in order to deal with the uneven illumination removal problem of text images and natural images simultaneously. Compared with the former ELBT method, the LLBT further improved the quality of uneven illumination removal for text images and a variant of LLBT can be used to process natural images. Unfortunately, the LLBT did not work well for natural images and failed to correct the illumination of text-photo images. In Ref. 3, the authors used human visual system-based multihistogram equalization to correct shadows and uneven LD of natural gray-level images. They separated the target image into regions by the quality of illumination and applied traditional histogram equalization on each region to correct for uneven illumination. However, their algorithm is somewhat complicated and needs to do image segmentation and fill the missing pixels. Also, their method is not suitable for text and text-photo images with uneven illumination. Lee et al.[4] proposed a method called "Sobel mechanism to determine text-photo object and design illumination-balance algorithm (SIBT)" for text and text-photo images in 2009. As for the performance of uneven illumination correction, the authors

*Address all correspondence to: Yu-Zhe Hsiao, E-mail: d99942011@ntu.edu.tw

0091-3286/2013/$25.00 © 2013 SPIE and IS&T

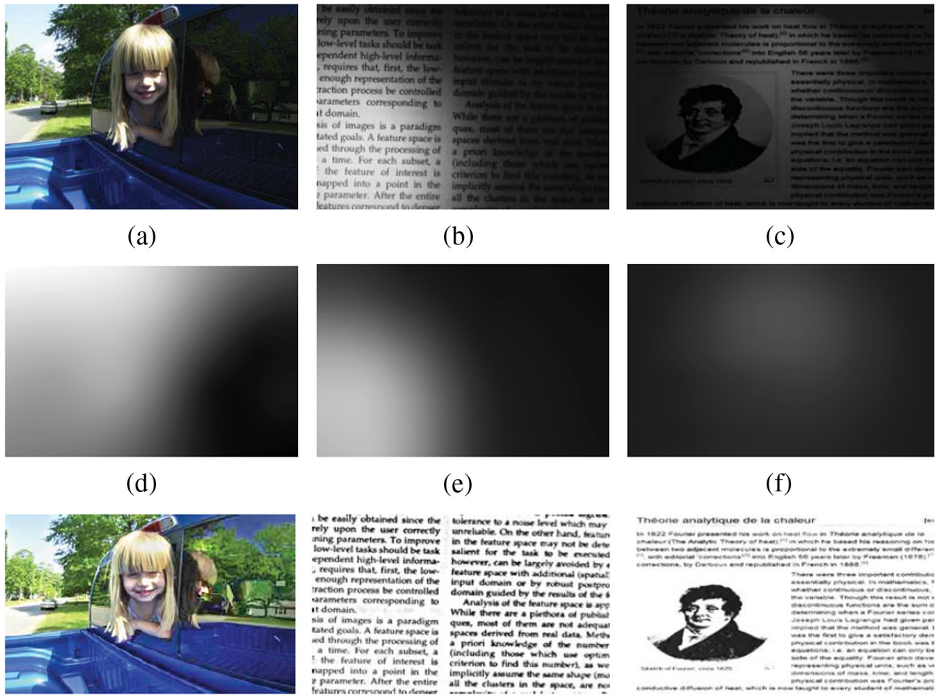

Fig. 1 First row: Images with uneven illumination. (a) Natural color image. (b) Text image. (c) Text-photo image. Second row: (d) (e) (f) are the estimated light distribution (LD) by line-based empirical mode decomposition (LBEMD) for (a), (b), and (c), respectively. Third row: (g) (h) (i) are the enhanced images by LBEMD for (a), (b), and (c), respectively.

claimed that the SIBT is better than ELBT and LLBT for text images and text-photo images.

However, the authors also mentioned that the SIBT is not suitable for full photo images, i.e., natural color/gray-level images. Also, in 2009, the authors[5] proposed a method based on morphology to balance the background illumination of poorly lighted natural gray-level images. Their method performs well in dealing with natural gray-level images with poor lighting. On the other hand, for image due to uneven illumination, their method usually fails to solve the problem. It cannot be used to process natural color images and the performance on text images is unsatisfactory. Recently, in 2010, Athimethphat and Patanavijit[6] proposed a technique called "nonlinear illuminations balancing for reconstructed degraded scanned text-photo image (NIBT)," which aimed to improve the inefficiency of SIBT for text-photo images. Compared with SIBT and LLBT, the algorithm showed that it achieved a slight improvement of uneven illumination correction in text images and text-photo images. However, the authors did not demonstrate the applicability of their method for natural color/gray-level images. The methods mentioned above (i.e., ELBT, SIBT, LLBT, NIBT, etc.) can only be used to correct uneven illumination problems of text or text-photo images. Contrary to these methods, in this article we propose a method based on empirical mode decomposition (EMD) to improve the performance of uneven illumination removal for text images, text-photo images, and natural color/gray-level images. The EMD is a powerful method for generating an adaptive multiscale structure of nonstationary signals and analyzing them.[7–9] There are several variations of the EMD algorithms introduced in Ref. 10. The EMD has recently been extended to analyze two-dimensional (2-D) signals,[11–14] and the extended version is called bidimensional empirical mode decomposition (BEMD). Intuitively, we should use the BEMD to process images (2-D signals). Indeed, we have developed an algorithm for uneven illumination removal based on BEMD in the first place. The performance of uneven illumination removal for natural color/gray level images is satisfactory. However, the processing speed of the BEMD is slow. Instead, we replace the BEMD by using one-dimensional line-based EMD (LBEMD) and average filter to enhance the processing speed. Detailed descriptions of the EMD algorithm and our method will be shown in the following sections. This paper is organized as follows. Section 2 describes the EMD algorithm. Section 3 presents the proposed method for text and text-photo images. Section 4 presents the method for natural color/gray-level images. Simulation results, comparison with other methods, and an EMD-based color constancy method are given in Sec. 5.

2 Empirical Mode Decomposition

The EMD was first introduced by Huang et al.[7] for signal processing. This novel tool decomposes nonlinear or nonstationary signals into frequency components called intrinsic mode functions (IMFs). The IMFs must satisfy the following two conditions:

- The number of extremes and the number of zero-crossings must either be equal or differ by one at most in the whole data set.
- At any point, the mean value of the envelope defined by the local maxima and the envelope defined by the

local minima is zero. The process of extracting an IMF from a signal is called the sifting process introduced in Ref. 7. We can extract IMFs from a real-valued signal $f(t)$ by the following steps:

1. Initialize $h_0(t) = r_0(t) = f(t)$, assume $i = j = 1$;
2. Identify all local maxima and minima of $h_{j-1}(t)$;
3. We generate the upper envelope by interpolating the local maxima, denoted $h_{\mathrm{upper}}(t)$, and the lower envelope by interpolating the local minima, denoted as $h_{\mathrm{lower}}(t)$;
4. Compute the envelope mean, $m_{j-1}(t) = [h_{\mathrm{upper}}(t) + h_{\mathrm{lower}}(t)]/2$;
5. Compute $h_j(t) = h_{j-1}(t) - m_{j-1}(t)$;
6. Repeat steps 2 to 5 and set $j = j + 1$ until $h_j(t)$ is an IMF;
7. $\mathrm{imf}_i(t) = h_j(t)$ and compute the i'th residue $r_i(t) = r_{i-1}(t) - \mathrm{imf}_i(t)$;
8. Repeat steps 2 to 7 and set $i = i + 1$ until $r_i(t)$ is monotonic. When $r_i(t)$ is monotonic, we have accomplished EMD, and set $r_L(t) = r_i(t)$. The original signal $f(t)$ can be expressed as the sum of IMFs $\mathrm{IMF}_i(t)$ and a final residue $r_L(t)$ as following equation:

$$f(t) = \sum_{i=1}^{L} \mathrm{IMF}_i(t) + r_L(t). \tag{1}$$

3 Line-Based EMD Method for Text and Text-Photo Images

Text and text-photo images are often printed in black over white paper, so the light source influences the text, photo, and background. We want to estimate the ratio of text and photo to background level and then adjust the background level to white. The EMD can decompose a signal into several IMFs and a final residue. The final residue is a monotonic slope. However, we do not necessarily need the final residue to represent the background level. Therefore, we do not carry out the sifting process until the residue is monotonic. In general, only three times is enough in our experience. Also, this simplified stop criterion of the EMD can reduce the computational cost and achieve good performance in removing uneven illumination.

It was shown in Ref. 8 that the last IMF may also be seen as a trend under certain conditions, though it is slightly oscillatory. Readers may wonder why we do not take the IMFs as our background level. The reason is that it may also be seen as a trend, but the mean value approximates to zero. Moreover, the very purpose of our method is to remove the uneven luminance, so we must use residue as the background level. In removing the uneven LD, the text or text-photo image is first decomposed by the EMD on rows and columns. This is the reason why we call it the LBEMD method. The operation of performing EMD on rows and columns of images was first used in Ref. 15. Interested readers may refer to Ref. 15 for more information. We take the average of row residue and column residue as the approximate LD. However, the residue obtained by averaging row residue and column residue is somewhat lacking in continuity. Therefore, we use an average filter with 30 pixels × 30 pixels mask to smooth the final residue. It should be noted that the size of the mask can be changed. We choose 30 pixels × 30 pixels mask because it works well for most of the natural color/gray-level images, text images, and text-photo images in our experience. The estimated LDs by using the LBEMD and average filter for Figs. 1(a)–1(c) are shown in Figs. 1(d)–1(f). We can see from Fig. 1 that the estimated LDs are satisfactory. After we obtain the smoothed residual image (the estimated LD), we can enhance text and text-photo images by the following equations:

$$R(x, y) = I(x, y)/r_L(x, y), \tag{2}$$

$$I'(x, y) = R(x, y) \times 255, \tag{3}$$

where $I(x, y)$ is the original pixel value, $r_L(x, y)$ is the estimated LD, $R(x, y)$ is the estimated reflectance, and $I'(x, y)$ is the modified pixel value. The purpose of Eq. (2) is to get the reflectance of the interested image by using Retinex theory. Retinex are image filters that can be used to enhance images taken in poor contrast situations. There are many Retinex filters proposed in literature, such as single scale Retinex (SSR), multi-scale Retinex (MSR), and multi-scale Retinex with color restoration (MSRCR).[16–20] The SSR and the MSR[19,20] are used to calculate the relative luminance

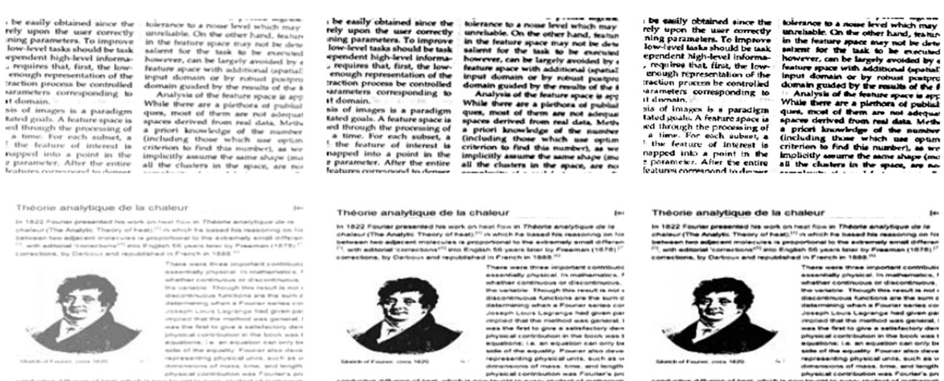

(a) (b) (c)

Fig. 2 Remove uneven illuminations in Fig. 1(b) and 1(c) by LBEMD algorithm with gain control. (a) $\alpha = 1$. (b) $\alpha = 2$. (c) $\alpha = 3$.

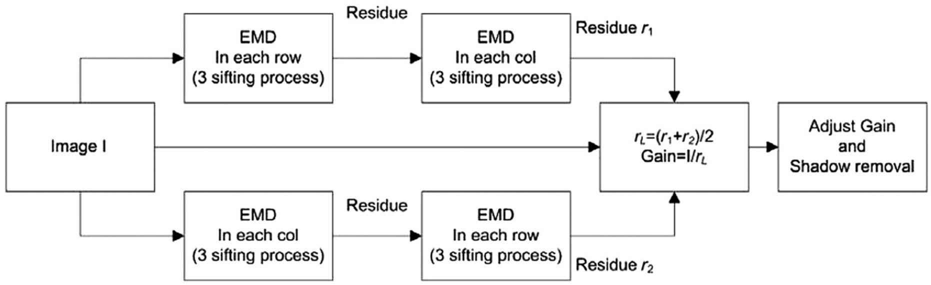

Fig. 3 The processing flow diagram of LBEMD for text and text-photo images.

Table 1 The LBEMD algorithm for text images, text-photo images and natural color/gray-level images, and the LBEMD color constancy algorithm for natural color images.

LBEMD algorithm for text and text-photo images

(1) Perform EMD on rows of input text image $I(x,y)$ and get the row residue $r_1(x,y)$;

(2) Perform EMD on columns of input text image $I(x,y)$ and get the column residue $r_2(x,y)$;

(3) Take the average of the row residue and column residue $r_L(x,y)$ as the approximate light distribution, where $r_L(x,y)=[r_1(x,y)+r_2(x,y)]/2$;

(4) Compute the reflectance $R'(x,y)$ of $I(x,y)$ by using $R'(x,y)=\alpha[I(x,y)/r_L(x,y)-1]+1$, where α is the gain used to control the darkness of texts. We smooth residue using average filter;

(5) Use the reflectance $R'(x,y)$ and white light source to get the relighted and uneven illumination removed text image $I'(x,y)$, where $I'(x,y)=R(x,y)\times 255$;

LBEMD algorithm for color/gray-level images

(1) Separate the luminance component $I(x,y)$ from nature color/gray-level image and keep the chrominance component $C(x,y)$ unchanged;

(2) Use LBEMD to decompose luminance component $I(x,y)$. After i'th sifting process, we can get IMFs and a temporary residue $L_i(x,y)$.

From retinex theory,[16–20] we know that $I(x,y)=L(x,y)\times R(x,y)$ where $I(x,y)$ is the luminance, $L(x,y)$ is the illumination and $R(x,y)$ is the reflectance. Each temporary residue $L_i(x,y)$ can be seen as the estimated light illumination in different scales;

(3) Then, the multiscale reflectance of the luminance image $I(x,y)$ can be estimated using the equation: $R_i(x,y)=I(x,y)/L_i(x,y)$;

(4) To remove shadow in dark regions and compress the dynamic range, we modify the estimated illumination as: $L_i'(x,y)=L_i(x,y)^\gamma$, where $L_i'(x,y)$ is the modified illumination of i'th scale and γ is the gamma compression ratio decided by the user to control the enhancement degree.

(5) Compute multiscale luminance $I_i'(x,y)$ by using

$I_i'(x,y)=R_i(x,y)L_i(x,y)^\gamma$;

(6) Combine all $I_i'(x,y)$ by using geometric mean, i.e., $I'(x,y)=\prod_{i=1}^{n} I_i'(x,y)^{1/n}$ to get the enhanced luminance component $I'(x,y)$ of original color image;

(7) Combine $I'(x,y)$ with $C(x,y)$ to get the enhanced color image, where $I(x,y)$ is the image, $L(x,y)$ is the illumination and $R(x,y)$ is the reflectance;

LBEMD color constancy algorithm for color images

(1) Compute the reflectances of three color channels:

$R_r(x,y)=I_r(x,y)/r_r(x,y)$

$R_g(x,y)=I_g(x,y)/r_g(x,y)$

$R_b(x,y)=I_b(x,y)/r_b(x,y)$

where $I_k(x,y)$ is the image of channel k, $R_k(x,y)$ is the reflectance of channel k, and $r_k(x,y)$ is the LBEMD residue of channel k ($k=$ red, green, blue);

(2) Finally, we relight these three channels using white light and get the color balanced image.

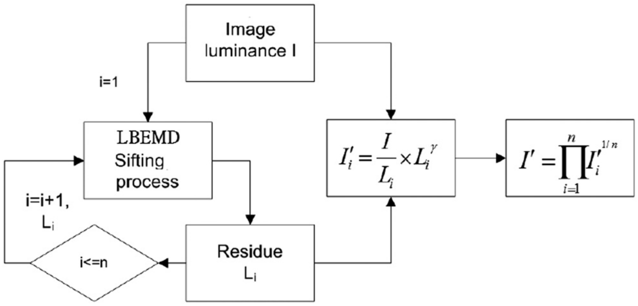

Fig. 4 The processing flow diagram of LBEMD for natural color/gray-level images.

between objects in gray-scale images. The MSRCR[18] is mainly used to compute relative chrominance between red, green, and blue channels in color images. In this article, we use Retinex theory to estimate the LD of uneven illuminated images. White light (value = 255 in black/white images) is used as background light source and we use the estimated reflectance $R(x, y)$ is to relight the text and text-photo images and remove the uneven illuminations, as shown in Eq. (3). The enhanced results of natural color image, text, and text-photo images are demonstrated in Figs. 1(g)–1(i). An advantage of the LBEMD over other similar methods (i.e., ELBT, LLBT, SIBT, NIBT, etc.) is that we can modify the darkness of the text and photo when the darkness of the enhanced text

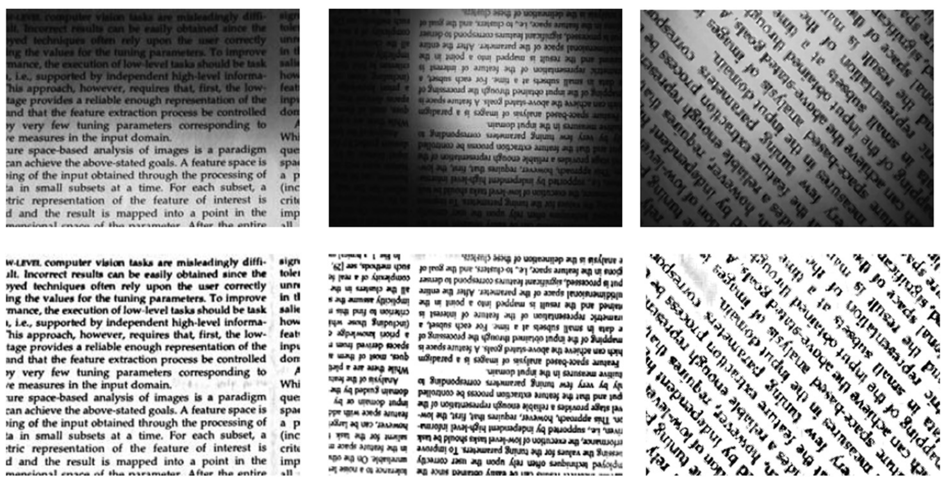

Fig. 5 First row: Text images with uneven illumination. Second row: Uneven illumination removal with proposed LBEMD method.

Fig. 6 Original image, uneven illuminated image, LD produced by Photoshop, estimated LD, and enhanced images by LBEMD. Peak signal-to-noise ratio (PSNR) is 17.03 dB for $\alpha = 1$ and 19.99 dB for $\alpha = 2$.

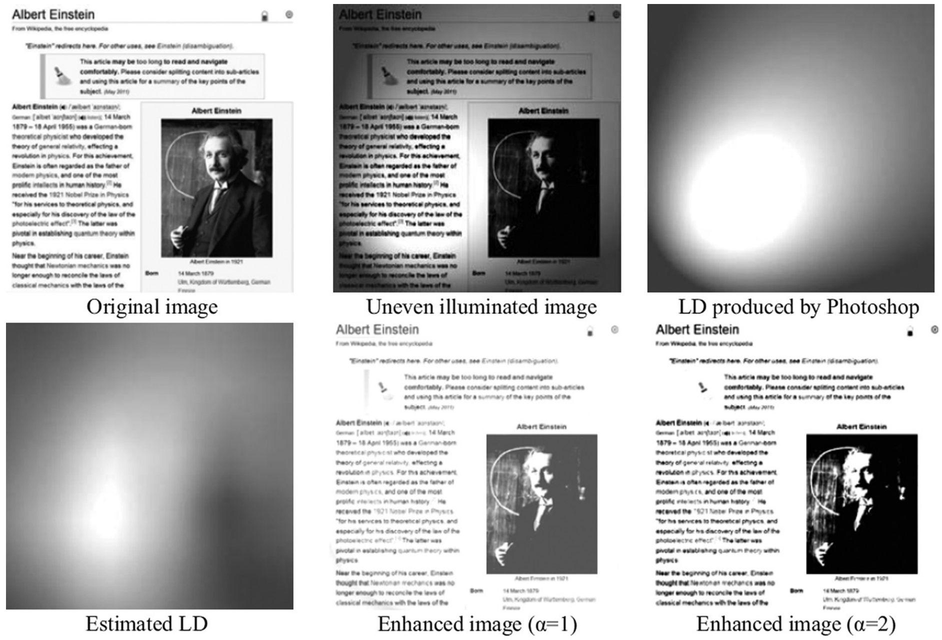

Fig. 7 Original image, uneven illuminated image, LD produced by Photoshop, estimated LD, and enhanced images by LBEMD. The PSNR is 18.00 dB for $\alpha = 1$ and 17.57 dB for $\alpha = 2$.

and photo is not enough to be readable. To achieve this goal, we modify Eq. (2) to the following equation to enhance the text and photo information:

$$R'(x, y) = \alpha[I(x, y)/r_L(x, y) - 1] + 1, \tag{4}$$

where α is the gain control of darkness. The value of α is determined by the user to control the clarity of text and photo content. We can make the content darker by setting a larger value of α since text and text-photo images are usually black-and-white. Figure 2 shows the enhanced results for Figs. 1(b) and 1(c) with $\alpha = 1$, 2, 3, and we can see that the clarity can be changed by adjusting gain. The processing flow diagram of the LBEMD for text and text-photo images is summarized in Fig. 3. The detailed algorithm is listed in Table 1. We will discuss more details about our method and demonstrate more experimental results (including comparison with other methods) in Sec. 5.

4 Line-Based EMD Method for Natural Color/Gray-Level Images

The LBEMD method can also be used to enhance natural color/gray-level images. Because the pleasing appearance

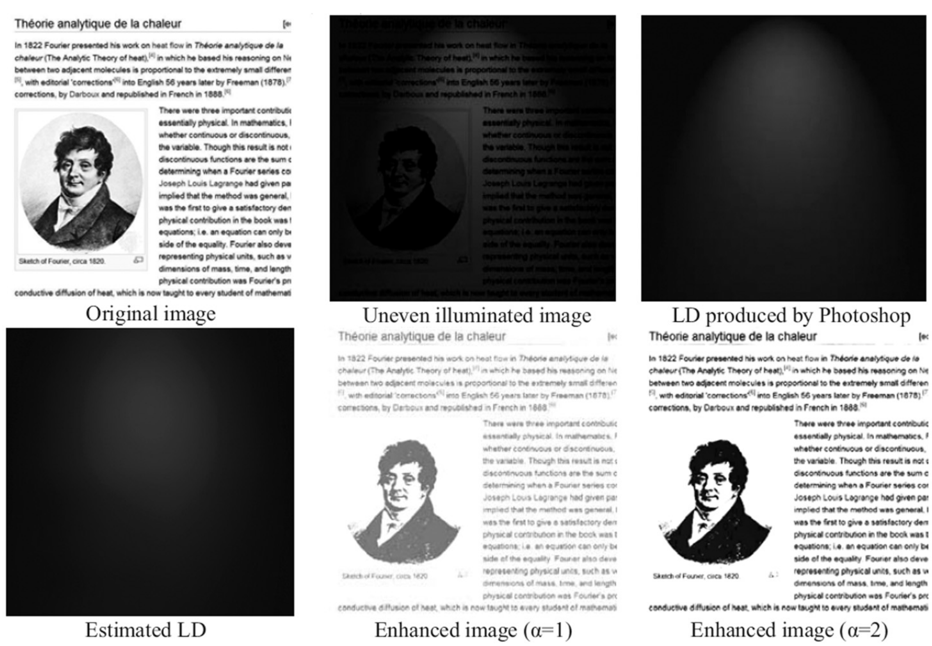

Fig. 8 Original image, uneven illuminated image, LD produced by Photoshop, estimated LD and enhanced images by LBEMD. The PSNR is 16.68 dB for $\alpha = 1$ and 20.30 dB for $\alpha = 2$. From Figs. 5–8, uneven illuminations are removed and we can adjust the darkness of text.

of the processed images instead of readability is the first concern when we deal with natural color/gray-level images, we slightly modified the equations in order to get more accurate LDs and reflectances. For color and gray-level images, we only process the luminance component separate from the image by using LBEMD, and for color images, we keep the chrominance component unchanged. Based on Retinex theory,[16–20] an image is composed of illumination and reflectance and it can be expressed as

$$I(x,y) = L(x,y) \times R(x,y), \tag{5}$$

where $I(x,y)$ is the image, $L(x,y)$ is the illumination, and $R(x,y)$ is the reflectance. After each sifting process, we can get IMFs and a temporary residue. We take each temporary residue as the estimated LD in n different scales. Then,

Table 2 The peak signal-to-noise ratio (PSNR) for enhanced text-photo images with different gains in Figs. 6–8.

Gain\PSNR	Fig. 6	Fig. 7	Fig. 8
$\alpha = 1$	17.03 dB	18.00 dB	16.68 dB
$\alpha = 2$	19.99 dB	17.57 dB	20.30 dB
$\alpha = 3$	18.09 dB	15.61 dB	16.82 dB

the multiscale reflectance of an image can be estimated using the following equation.

$$R_i(x,y) = I(x,y)/L_i(x,y) \quad i = 1 \text{ to } n. \tag{6}$$

In other words, the original image divided by the residual image corresponds to the reflectance. To remove shadows in dark regions and compress the dynamic range, modified illumination is

$$L_i'(x,y) = L_i(x,y)^\gamma, \tag{7}$$

where L_i' is the modified illumination of the i'th scale and γ is the gamma compression ratio decided by the user to control the enhancement degree. Then, each modified image can be expressed as

$$I_i'(x,y) = R_i(x,y)L_i(x,y)^\gamma \tag{8}$$

and we combine all scales of the modified image using geometric mean, as in the following equation:

$$I'(x,y) = \prod_{i=1}^{n} I_i'(x,y)^{1/n}, \tag{9}$$

where $I'(x,y)$ is the modified pixel value. The processing flow diagram for uneven illumination removal of color/

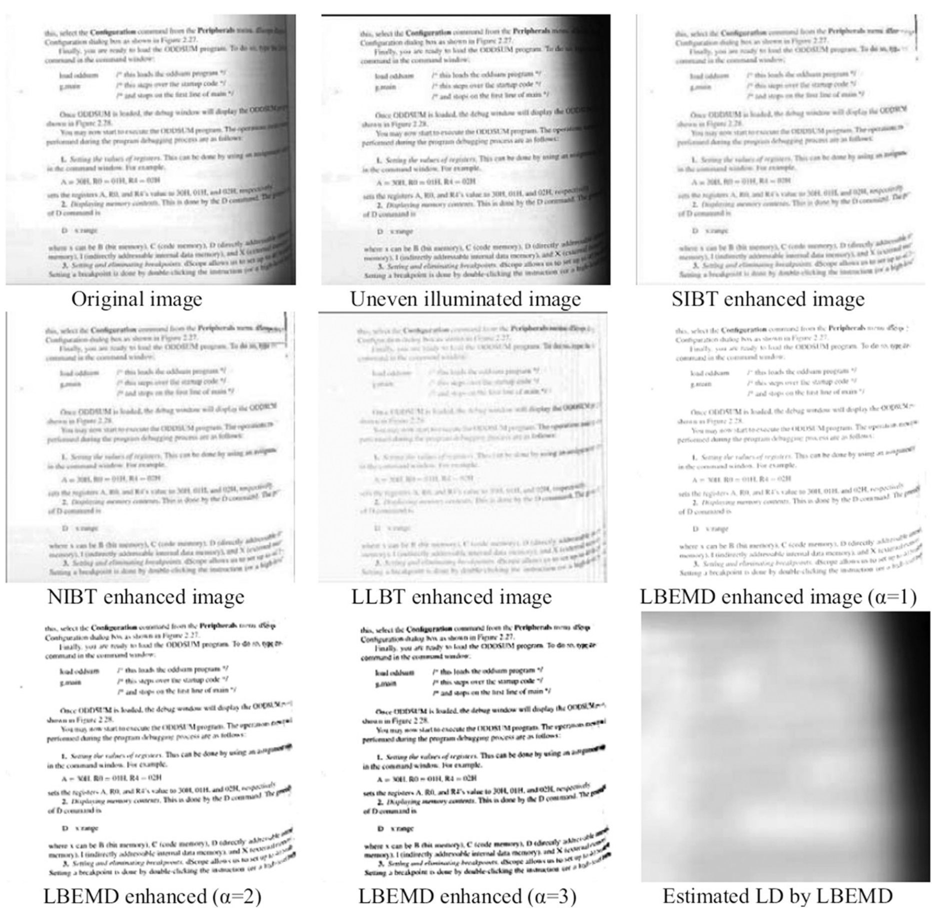

Fig. 9 Comparison of LBEMD and other methods (SIBT, NIBT, and LLBT) for text image. The enhanced text parts by using our method are clearer. The darkness of text can be adjusted.

Table 3 The PSNR comparison of LBEMD and other current methods (SIBT, NIBT, and LLBT) for text image.

Method\Gain	$\alpha = 1$	$\alpha = 2$	$\alpha = 3$
SIBT	13.82 dB	NA	NA
NIBT	13.94 dB	NA	NA
LLBT	14.08 dB	NA	NA
LBEMD	19.76 dB	19.13 dB	18.58 dB

gray-level images is summarized in Fig. 4. The algorithm is listed in Table 1.

5 Experimental Results

5.1 *For Text and Text-Photo Images*

In order to demonstrate the performance of our algorithm, we take several text and text-photo images with light sources on different sides to test our method. The uneven illuminations are generated by using image processing software Photoshop. For text images, the enhanced results by the LBEMD method are demonstrated in the second row of Fig. 5. Since the EMD is adapted locally according to image data, the proposed method can automatically compute the ratio of text to background level by Eq. (2) and use Eq. (3) to adjust the background level to white. The number of iterations in each sifting process is five, and the number of sifting processes is three for each LBEMD in our experiment. These experimental results show that our algorithm can remove the uneven illumination effectively, no matter where the illuminant is, and turn the background of the text images to white. This is true even when the text is not arranged horizontally, but is rotated by some angle, e.g., 135 deg, as the bottom right of second row of Fig. 5 shows. The proposed method still works well and demonstrates its robustness. For text-photo images, we further demonstrate the original LD generated by Photoshop and compare it with the estimated LD by LBEMD. As can be seen in Figs. 6–8, our method can effectively estimate the LD and remove uneven illumination.

Fig. 10 Comparison of our LBEMD and other methods for text-photo image. The enhanced text parts by using our method are clearer. The darkness of text can be adjusted and the photo parts are best corrected.

The darkness control by adjusting gain in Eq. (4) is possible. We use peak signal-to-noise ratio (PSNR) as performance index for the enhanced images. The PSNR results for enhanced text-photo images with different gains ($\alpha = 1$ to $\alpha = 3$) in Figs. 6–8 are summarized in Table 2.

Finally, we compare our LBEMD method with recently proposed methods (i.e., SIBT, LLBT, and NIBT) by using the test images from Ref. 6. For text image, as can be seen from Fig. 9 and Table 3, the PSNR of LBEMD is higher than those of SIBT, LLBT, and NIBT. The text parts in SIBT-, LLBT-, and NIBT-enhanced images are somewhat blurred. The text part obtained by using LBEMD is more clear and readable than those of SIBT, LLBT, and NIBT. Moreover, we also have the advantage of controlling text clarity by using LBEMD. For text-photo image, as can be seen from Fig. 10 and Table 4, the PSNR of LBEMD is also better than those of SIBT, LLBT, and NIBT. As for the appearance of enhanced images, the text part obtained by using LBEMD is still more clear and readable than SIBT, LLBT, and NIBT. The enhanced photo part of LBEMD outperforms SIBT, LLBT, and NIBT. All in all, the LBEMD can enhance text and text-photo images effectively and the performance is better than recently proposed similar methods. We implement the LBEMD and other methods using MATLAB and the average run time of our program is listed in Table 5 (for text images and text-photo images). The size of text and text-photo images in this article are scaled to 300 pixels × 300 pixels in MATLAB and we use Intel Pentium 4, 3 GHz CPU, and 1 GB DDR RAM to run our program.

5.2 *For Natural Color and Gray-Level Images*

Unlike text images, it is more difficult to address the uneven illumination problem for natural images because the reflectance from object to object in the image will influence each other. It is not enough to estimate only one light source scale, so we use the multiscale structure to decompose color images. The LBEMD is like a low-pass filter, in that it can adaptively separate the details from the image and get the residue with low frequency. Because we want to preserve the original color component, we convert the color space from RGB to HSV and apply our algorithm to V, which is the luminance component. Because we only operate LBEMD on the luminance component of an image, our method can process the color image and the gray-level image simultaneously. After removing the uneven LD of the luminance component, we convert HS with modified V back to RGB color space. The enhanced results of natural color images are demonstrated in Fig. 11 with $n = 3$ (scale), and $\gamma = 0.25$ (gamma compression ratio). We also utilize the well known Yale Face Database B[21] to test our method for natural gray-level images. The Yale Face Database B contains 5760 single light source images of 10 subjects each seen under 576 viewing conditions (9 poses × 64 illumination conditions). The comparison of the original face images with the uneven illuminations removed images is demonstrated in Fig. 12 with $n = 3$, $\gamma = 0.25$. It can be seen from the figure that the uneven illuminated image are enhanced and we think that our method can be applied to face recognition tasks

Table 4 The PSNR comparison of LBEMD and other current methods (SIBT, NIBT, and LLBT) for text-photo image.

Method\Gain	$\alpha = 1$	$\alpha = 2$	$\alpha = 3$
SIBT	15.16 dB	NA	NA
NIBT	17.60 dB	NA	NA
LLBT	14.35 dB	NA	NA
LBEMD	19.93 dB	19.29 dB	18.74 dB

Table 5 Average run time of LBEMD and other methods for text and text-photo images. [Average run time = (Fig. 9 run time + Fig. 10 run time)/2. All images are scaled to 300 × 300 pixels in MATLAB under Intel Pentium 4, 3 GHz CPU, and 1 GB DDR RAM].

Avg. run time	$\alpha = 1$	$\alpha = 2$	$\alpha = 3$
SIBT	9.85 s	NA	NA
NIBT	8.25 s	NA	NA
LLBT	4.38 s	NA	NA
LBEMD	5.56 s	5.56 s	5.56 s

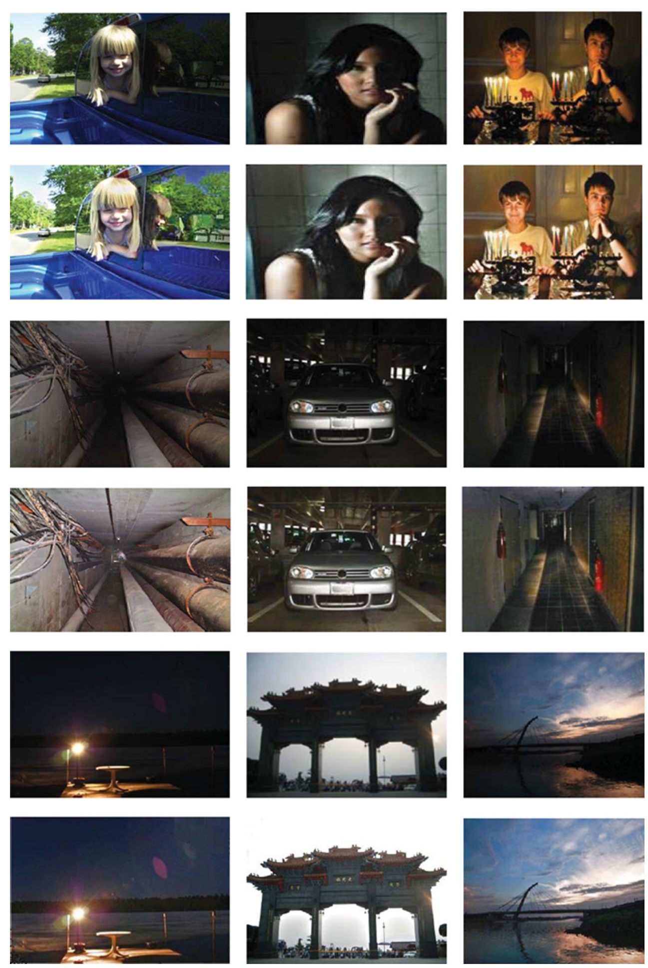

Fig. 11 Odd rows: Natural color images with uneven illumination. Even rows: uneven illumination removal with LBEMD algorithm. Uneven illuminations are removed effectively.

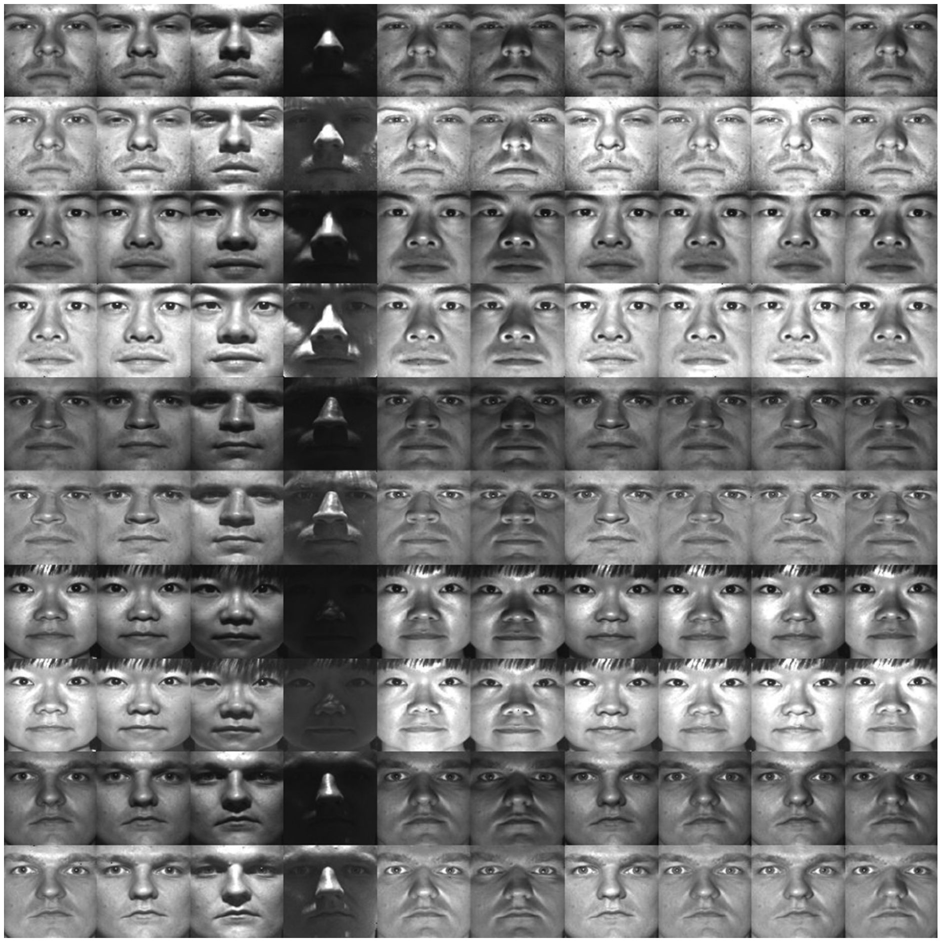

Fig. 12 Comparison of face images under uneven illuminations (in odd rows) with the uneven illuminations removed images (in even rows) using LBEMD. Only parts of the results (five subjects each seen under ten viewing conditions) are shown because of the space limitation.

and help increase the face identification rate. From these experimental results, it is obvious that our approach can effectively improve uneven illumination and contrast. We will apply our method to face recognition method like Du and Ward[22] did to verify the efficacy of our method in the future.

When an image is influenced by poor lighting and uneven illumination simultaneously, our approach still performs well. Recently, the authors[5] proposed a method using morphological background detection for enhancement of images with poor lighting. They demonstrated the superiority of their method in dealing with images with poor lighting. However, when poorly lighted images are obtained due to uneven illumination, their method usually fails to tackle the problem. As Fig. 13(b) shows, although the poorly lighted part on the right side of the image is enhanced, the well lighted left side is overenhanced. The histogram equalization method fails to deal with the test image well because of the local low contrast, as Fig. 13(c) demonstrates. The resultant image in Fig. 13(d) obtained by applying our method shows that the uneven illumination is removed, and the scene is relighted naturally. For text images, similar results can be seen in Fig. 14. Our method eliminates uneven illumination successfully and demonstrates the text parts clearly, whereas the other two methods yield inferior results. Figure 15 depicts the results by applying our approach to the poorly lighted images from Ref. 5 and the results by performing the approach of Ref. 5 and histogram equalization. The histogram equalization performs slightly better in this case because of the global low contrast of test image.

(a) (b) (c) (d)

Fig. 13 (a) Image influenced by poor lighting and uneven illumination. (b) Enhance (a) using Ref. 5. (c) Enhance (a) by using histogram equalization. (d) Enhance (a) by using our approach.

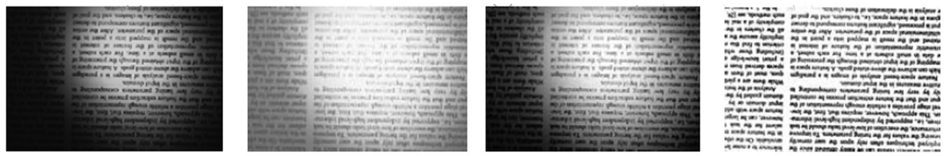

(a) (b) (c) (d)

Fig. 14 (a) Image influenced by poor lighting and uneven illumination. (b) Enhance (a) by using Ref. 5. (c) Enhance (a) by using histogram equalization. (d) Enhance (a) by using our approach.

These figures show that our approach can not only deal with uneven illumination but can also perform well under poor lighting conditions or when the above factors are combined together. The images are enhanced more naturally and are more visually pleasing when using our method, demonstrating the robustness and superiority of our approach under different lighting conditions in natural environments.

5.3 *Color Constancy*

Color constancy[17] is often required in many image processing fields, such as computer vision, image enhancement, pattern recognition, etc. There are numerous color constancy approaches proposed in the literature. All of them suppose that there is only a single light source and the light color is spatially uniform across the scene. The color of the scene illumination is first estimated and then the original image will be color-corrected by the Von Kries model.[23] The two most widely used groups of illuminant estimation approaches are low level statistics-based techniques, which are underlying the assumptions of the pixel values or pixel differences (derivatives) distribution in the scene and the gamut-based measures. Gray World (GW),[24] White Patch Retinex (WPR),[25] General Gray World (GGW),[26] Shades of Gray (SoG),[27] first order Gray Edge (GE1), and second order Gray Edge (GE2)[26] all belongs to the first group and the second group contains pixel-based gamut mapping (PBGM),[28] edge-based gamut mapping (EBGM), and intersection-based gamut mapping (IBGM).[29] The Retinex theory[17] based method takes the RGB values of each pixel of the image as input and attempts to estimate the reflectances of each point. The maximal red value $r_{\max}$, green value $g_{\max}$, and blue value $b_{\max}$ of all pixels are calculated. The illuminating light source is described by ($r_{\max}$, $g_{\max}$, $b_{\max}$). For each pixel, its reflectance is estimated as ($r/r_{\max}$, $g/g_{\max}$, $b/b_{\max}$). Inspired by the Retinex theory-based method, we propose a LBEMD-based color constancy method that applies LBEMD to three color channels (RGB) separately and we use the residues obtained to estimate the reflectances of each channel respectively. The reflectances of three color channels can be computed by the following formula:

$$R_r(x,y) = I_r(x,y)/r_r(x,y), \quad R_g(x,y) = I_g(x,y)/r_g(x,y),$$
$$R_b(x,y) = I_b(x,y)/r_b(x,y), \tag{10}$$

where $I_k(x,y)$ is the image of channel k ($k=$ red, green, blue), $R_k(x,y)$ is the reflectance of channel k, and $r_k(x,y)$ is the LBEMD residue of channel k. Finally, we relight these three channels using white light and the estimated

(a) (b) (c) (d)

Fig. 15 (a) Image influenced by poor lighting. (b) Enhance (a) by using Ref. 5. (c) Enhance (a) by using histogram equalization. (d) Enhance (a) by using our approach. From Figs. 13–15, our method enhances image naturally and can process text image effectively.

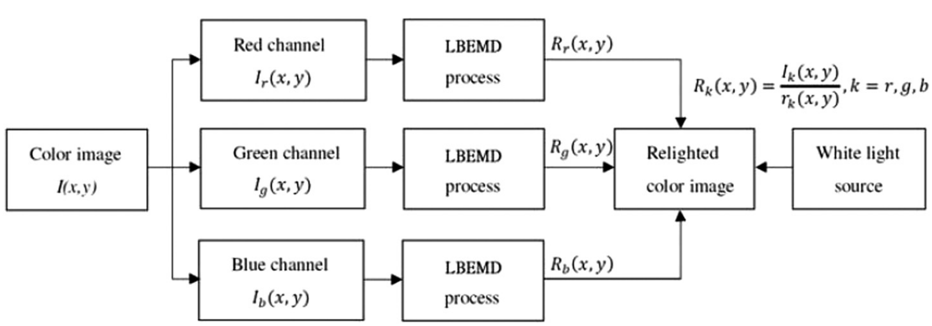

Fig. 16 The processing flow diagram for proposed color constancy method.

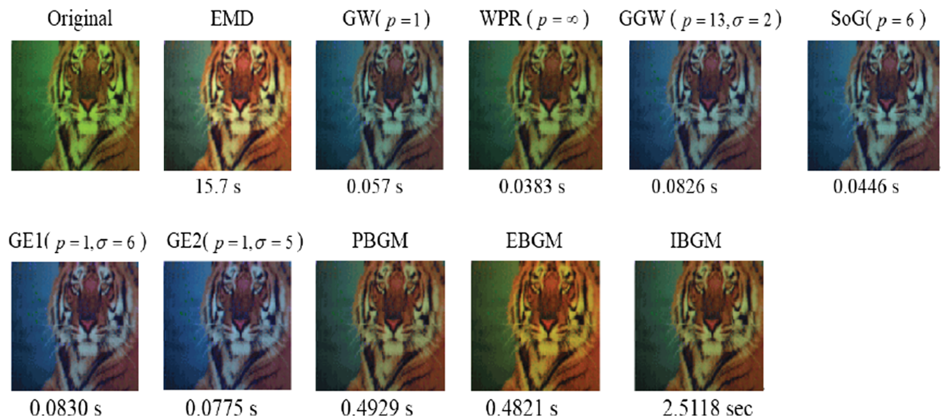

Fig. 17 Comparison of LBEMD color constancy method and other methods. Test image: Tiger.

Fig. 18 Comparison of LBEMD color constancy method and other methods. (a) Test image: Fruits. (b) Test image: Street. It can be seen that our method outperforms other methods.

Fig. 19 Comparison of LBEMD color constancy method and other methods. Test image: Singer. It can be seen from Figs. 17–19 that our method outperforms other methods in appearance and corrects the colors well. The recovered images are more natural and pleasing.

reflectances to correct poorly lighted color images. In this way, we accomplish the color constancy tasks. Figure 16 depicts the processing flow diagram of our method. The LBEMD approach directly calibrates the color deviation and does not require estimating the illuminant in the scene. It implies that this method may be applied to the case of multiple and nonuniform light sources, i.e., the illuminant received for each pixel can be different. Furthermore, it is not limited by the assumption of the image statistics and does not need a training process, which is important for the gamut mapping techniques. In Figs. 17–19, we use four test images with different color casts to compare the proposed LBEMD algorithm with all of above mentioned algorithms. The parameters of GGW, SoG, GE1, and GE2 are set according to the heuristics.[26] In Fig. 17, we can see from the fur of the tiger that the color cast is greenish. The corrected results of the proposed LBEMD, PBGM, and IBGM are the best since the white part of the fur indeed looks white and the yellow part is also enhanced. On the other hand, the WPR cannot alleviate the color cast and the outcome still looks greenish. For EBGM, the white part of the fur looks greenish even though the yellow part is improved. Finally, the results of GW, GGW, SoG, GE1, and GE2 look somewhat bluish. For Fig. 18(a), the primary goal is to remove the greenish color cast and reconstruct the real colors of the fruits. It is obvious to see that the yellow color of the banana is seriously polluted and therefore, we can determine the goodness of a color constancy algorithm by the enhanced level of the banana. The proposed LBEMD method improves the banana strongest and most pleasurably, because the saturation of the color corrected image is the best. The outcomes of GW, GGW, SoG, and GE1 look a little bluish. Although GE2 and the gamut mapping-based methods also perform very well, the corrected images are less colorful than that of the EMD. It is clear to see that LBEMD effectively removes the bluish color cast in Fig. 18(b). The place near the street light is too reddish in the corrected image for GW. All results of other algorithms still look bluish. There is an apparent color cast in Fig. 19. The LBEMD restores the colors of the skin and the hair pretty well. The resultant color corrected images of all other color constancy schemes except for PBGM and IBGM, which perform worse, still look a little reddish. The average run time of LBEMD as well as all other color constancy methods for the above four example images are illustrated in Table 6. It can be seen that the run time of LBEMD is slower than other methods. This is because the LBEMD algorithm needs to do many iterations and therefore, many loops when the size of the test image is large. The MATLAB is not suitable and is inefficient for programs with loops. We adopt it to test our method because many color constancy methods mentioned above are implemented using MATLAB. The computational speed for LBEMD can be significantly increased by using other programming languages like C++ and by using the parallel processing technique mentioned in Ref. 30.

Table 6 Average run time of line-based empirical mode decomposition (LBEMD) color constancy method and other methods. Test image sizes: Tiger (112×131 pixels), Fruits (88×145 pixels), Street (120×160 pixels), and Singer (103×160 pixels).

Method	EMD	GW	WPR	GGW	SoG	GE1	GE2	PBGM	EBGM	IBGM
Average run time (s)	14.68	0.056	0.038	0.083	0.045	0.084	0.079	0.672	0.682	4.272

6 Conclusion

In this article, a novel algorithm called LBEMD for uneven illumination removal in images is proposed based on EMD. The LBEMD can be used to correct text image, text-photo images, and natural color/gray-level images. Furthermore, a LBEMD-based color constancy method is proposed to correct poorly-lighted color images, and we obtained satisfactory results as seen from Figs. 17–19. The experimental results demonstrate that the proposed technique can effectively improve LD for text image, text-photo images, and natural color/gray-level images. This technique is valuable for improving the quality of images with poorly lighted distribution.

References

1. S. C. Hsia and P. S. Tsai, "Efficient light balancing techniques for text images in video presentation system," *IEEE Trans. Circuits Syst. Video Technol.* **15**(8), 1026–1031 (2005).
2. S. C. Hsia and P. S. Tsai, "A cost-effective line-based light balancing technique using adaptive processing," *IEEE Trans. Image Process.* **15**(9), 2719–2729 (2006).
3. E. Wharton, K. Panetta, and S. Agaian, "Human visual system based multi-histogram equalization for nonuniform illumination and shadow correction," in *ICASSP*, pp. I.729–I.732, IEEE Signal Processing Society, Honolulu, Hawaii (2007).
4. J.-S. Lee, C.-H. Chen, and C.-C. Chang, "A novel illumination-balance technique for improving the quality of degraded text-photo images," *IEEE Trans. Circuits Syst. Video Technol.* **19**(6), 900–905 (2009).
5. A. R. Jiménez-Sánchez et al., "Morphological background detection and enhancement of images with poor lighting," *IEEE Trans. Image Proces.* **18**(3), 613–623 (2009).
6. M. Athimethphat and V. Patanavijit, "A non-linear illuminations balancing for reconstructed degraded scanned text-photo image," in *Int. Symp. Commun. Inf. Technol. (ISCIT)*, pp. 1158–1163, IEEE Circuits and Systems (IEEE-CAS) Society, Tokyo, Japan (2010).
7. N. E. Huang et al., "The empirical mode decomposition and hilbert spectrum for nonlinear and nonstationary time series analysis," *Proc. Roy. Soc. London A* **454**(1971), 903–995 (1998).
8. G. Rilling, P. Flandrin, and P. Goncalves, "Empirical mode decomposition as a filter bank," *IEEE Signal Process. Lett.* **11**(2), 112–114 (2004).
9. G. Rilling, P. Flandrin, and P. Goncalves, "Detrending and denoising with empirical mode decomposition," in *EUSIPCO*, pp. 1581–1584, EURASIP, the European Association for Signal, Speech, and Image Processing, Vienna, Austria (2004).
10. G. Rilling, P. Flandrin, and P. Goncalves, "On empirical mode decomposition and its algorithms," in *IEEE-EURASIP Workshop on Nonlinear Signal and Image Processing NSIP-03*, The European Association for Signal Processing, Grado, Italy (2003).
11. A. Linderhed, "Compression by image empirical mode decomposition," proceedings of international conference on image processing," in *ICIP-05*, pp. 553–556, IEEE Signal Processing Society, Genoa, Italy (2005).
12. A. Linderhed, "2D empirical mode decompositions in the spirit of image compression," *Proc. SPIE* **4738**, 1–8 (2002).
13. J. C. Nunes et al., "Image analysis by bidimensional empirical mode decomposition," *Image Vis. Comput.* **21**(12), 1019–1026 (2003).
14. J. C. Nunes, S. Guyot, and E. Deléchelle, "Texture analysis based on local analysis of the bidimensional empirical mode decomposition," *Mach. Vis. Appl.* **16**(3), 177–188 (2005).
15. Z. Liu, H. Wang, and S. Peng, "Texture segmentation using directional empirical mode decomposition," in *ICIP*, pp. 279–282, IEEE Signal Processing Society, Singapore (2004).
16. D. J. Jobson, Z. Rahman, and G. A. Woodell, "Properties and performance of a center/surround retinex," *IEEE Tran. Image Process.* **6**(3), 451–462 (1997).
17. E. Land and J. McCann, "Lightness and retinex theory," *J. Opt. Soc. Am.* **61**(1), 1–11 (1971).
18. D. Jobson, Z.-U. Rahman, and G. Woodell, "A multiscale retinex for bridging the gap between color images and human observation of scenes," *IEEE Trans. Image Process.* **6**(7), 965–976 (1997).
19. Z.-U. Rahman, D. Jobson, and G. Woodell, "Multi-scale retinex for color image enhancement," in *Int. Conf. Image Process.*, Vol. 3, pp. 1003–1006 (1996).
20. Z.-U. Rahman, D. Jobson, and G. Woodell, "Retinex processing for automatic image enhancement," *J. Electron. Imaging* **13**(1), 100–110 (2004).
21. A. S. Georghiades, P. N. Belhumeur, and D. J. Kriegman, "From few to many: illumination cone models for face recognition under variable lighting and pose," *IEEE Trans. Pattern Anal. Mach. Intell.* **23**(6), 643–660 (2001).
22. S. Du and R. Ward, "Adaptive region-based image enhancement method for robust face recognition under variable illumination conditions," *IEEE Trans. Circuits Syst. Video Technol.* **20**(9), 1165–1175 (2010).
23. K. Barnard et al., "A comparison of computational color constancy algorithms part ii: experiments with image data," *IEEE Trans. Image Process.*, pp. 985–996 (2002).
24. G. Buchsbaum, "A spatial processor model for object color perception," *J. Frank. Inst.* **310**(1), 1–26 (1980).
25. E. H. Land, "The retinex theory of color vision," *Sci. Am.* **237**(6), 108–128 (1977).
26. J. van de Weijer, T. Gevers, and A. Gijsenij, "Edge-based color constancy," *IEEE Trans. Image Process.* **16**(9), 2207–2214 (2007).
27. G. D. Finlayson and E. Trezzi, "Shades of gray and color constancy," in *Proc. IS&T/SID 12th Color Imaging Conf.*, pp. 37–41, IS&T-Society for Imaging Science and Technology, Scottsdale, AZ (2004).
28. D. Forsth, "A novel algorithm for color constancy," *Int. J. Comput. Vis.* **5**(1), 5–36 (1990).
29. A. Gijsenij, T. Gevers, and J. van de Weijer, "Generalized gamut mapping using image derivative structures for color constancy," *Int. J. Comput. Vis.* **86**(2–3), 127–139 (2010).
30. L.-W. Chang et al., "Parallel implementation of multi-dimensional ensemble empirical mode decomposition," in *36th Int. Conf. Acoust., Speech, and Signal Process. (ICASSP)*, IEEE Signal Processing Society, Prague Congress Centre Prague, Czech Republic (2011).

Soo-Chang Pei received his PhD degree from the University of California, Santa Barbara, in 1975, in electrical engineering. His research interests include digital signal processing, image processing, optical information processing, and laser holography. He received the IEEE fellow in 2000 for contributions to the development of digital eigenfilter design. He is a member of Eta Keppa Nu and the Optical Society of America.

Yu-Zhe Hsiao received his MS degree from the National Taiwan University, 2010, in communication engineering. His research interests include empirical mode decomposition, image processing, quaternion, and reduced biquaternion signal processing.

Mary Tzeng received her MS degree from the National Taiwan University, 2007, in communication engineering. Her research interests include empirical mode decomposition, image processing, and digital signal processing.

Feng Ju Chang received her MS degree from the National Taiwan University, 2011, in communication engineering. Her research interests include white balancing of images, image processing, and enhancement.